

Two-Stage Melting in Dilute Gels of Poly(γ -benzyl L-glutamate)Yoshinobu Izumi,^{*,†} Hikaru Takezawa,[†] Noriyuki Kikuta,[†] Soichi Uemura,[†] and Akihiro Tsutsumi[‡]*Human Sensing and Functional Sensor Engineering, Graduate School of Engineering, Yamagata University, Yonezawa 992, Japan, and Department of Applied Physics, Graduate School of Engineering, Hokkaido University, Sapporo 060, Japan**Received June 12, 1997; Revised Manuscript Received September 16, 1997*

ABSTRACT: Two-stage melting of the dilute gels of poly(γ -benzyl L-glutamate) in benzene has been studied by differential scanning calorimetry, wide-angle X-ray diffraction, and small-angle X-ray scattering using synchrotron radiation. Differential scanning calorimetry measurements show that the traces on heating exhibit two endothermic peaks at about 25 °C and at about 31 °C, thereby indicating the melting of two types of aggregates, while those on cooling exhibit no exotherm even at 0 °C, thereby indicating a large thermal hysteresis. Wide-angle X-ray diffraction measurements show that the profiles yield little of interest other than diffuse halos from the solvent except a diffuse small-angle scattering, thereby indicating that the aggregates do not contain a solid crystalline phase but a crystal–solvent phase. Small-angle X-ray scattering measurements show that the two-stage melting of the aggregates can be attributed to a melting first of the bundles of three rods and then of the bundles of two rods and that, above the two-stage melting temperature, the gels transform into the dilute and isotropic solutions, in which the poly(γ -benzyl L-glutamate) stiff chains are randomly dispersed and do not interact with each other. We suggest that the intermolecular interactions causing the bundles to aggregate are induced by the solvent.

Introduction

It is well-known that poly(γ -benzyl L-glutamate) (PBLG) forms aggregates in very dilute solutions of some helicogenic poor solvents such as benzene, toluene, mixed solvents of dioxane with fatty acids, or benzyl alcohol^{1–7} and thermoreversibly gels above some critical concentration.^{8–17} Although the aggregation can be characterized by the side-by-side and head-to-tail types, and their combinations, its role in gelation has not been well-understood. In this paper, we focus our attention on the gelation of dilute solutions, because that of concentrated solutions exhibits a complex behavior. In particular, we are interested in revealing the mechanism of a two-stage melting observed in the dilute gels of PBLG in the dioxane/water and benzene systems,¹² because microcellular foam materials prepared from the gels have the potential for many applications such as filters, controlled release media, catalytic substrates, artificial skin and blood vessels, and three-dimensional reinforcements for composites.

Jackson and Shaw attributed the two-stage melting to a melting first of crystals and then of the liquid crystalline (LC) phase.¹² They discuss the relationship between phase separation and gelation and suggest that phase separation is occurring by nucleation and growth rather than spinodal decomposition, over the concentration range they consider. However, it has been pointed out that the appearance of the two-stage melting is puzzling, taking into account crystals identified only by a single melting endotherm in the differential scanning calorimetry (DSC).¹³ Furthermore, these authors also presented another possible explanation based on the observed foam morphology.¹² However, the form morphology may be greatly influenced by the solvent

removal after gelation. No one knows to what extent the drying process modifies the gel nascent structure. Therefore, in order to reveal the mechanism, it is desirable that various measurements containing some novel experimental techniques are performed on the nascent state.

Present study is aimed at understanding the mechanism of the two-stage melting of the dilute gels of PBLG in benzene. We first explore further evidences on the two-stage melting applying following nondestructive techniques to the nascent gels: DSC, wide-angle X-ray diffraction (WAXD), and small-angle X-ray scattering using synchrotron radiation (SR–SAXS) measurements. We discuss the mechanism of the two-stage melting of the gels from the view-point of dissociation of the assembly of parallel rods.

Experimental Section

Materials. The sample of PBLG was synthesized by the *N*-carboxy anhydride method using triethylamine as the initiator in dioxane.¹⁸ The sample was recovered by precipitating with ethanol and drying in vacuo. Molecular weight was determined from the intrinsic viscosity in dichloroacetic acid using the relation given by Doty et al.¹ The viscosity average molecular weight of PBLG is about 33×10^4 . The benzene was guaranteed reagent grade from Kanto Chemical Co. and purified. The gel samples were prepared by quenching into cold water above the freezing point of benzene after dissolving at 90 °C for 2–3 days.

DSC Measurements. Transition temperatures and heats of transition were determined by means of a Seiko DSC 120 instrument equipped with a thermal analysis data station.¹⁹ It is reported that this calorimeter is perhaps 10 times more sensitive than calorimeters commonly used for bulk polymers.¹⁷ DSC pans specially designed for liquids were used, and sample weights were approximately 50 mg. The pans were weighted before and after testing to assure that solvent was not lost. The DSC measurements were carried out at a constant rate of 0.25 °C/min. The concentrations of PBLG were prepared in the range 0.5–7.7 wt %.

WAXD Measurements. The WAXD measurements were performed on a MAC Rotating Anode (M18XHF-SRA) at 50kV

* To whom correspondence should be addressed. Fax: 0238-26-3177. E-mail: yizumi@dp.yz.yamagata-u.ac.jp.

[†] Yamagata University.

[‡] Hokkaido University.

and 300mA using Cu K α radiation. The range of the scattering vector, h , equals to $(4\pi/\lambda) \sin \theta$ was 0.8–25 nm $^{-1}$, where λ is the wavelength used and 2θ is the scattering angle. Exposure time of 1200 s was used. The diffracted X-ray signal was detected by using a MAC imaging plate system (DIP220). The diffraction angle was calibrated by measuring the WAXD pattern of NaCl as a standard. The sample was sealed in a 3-mm-thick plate cell with mica windows of 15 μ m thick. The concentration of PBLG, i.e., 20 wt %, was selected because it is necessary to increase the concentration of dilute gels in order to allow a distinction between solid crystalline or crystal-solvate phase, considering the fact that the WAXD patterns of dilute gels are smeared out by the scattering from the solvent.¹⁰ The temperature range was 15–70 $^{\circ}$ C, and each temperature indicated a constant temperature within 0.01 $^{\circ}$ C.

SR-SAXS Measurements. The application of the SR-SAXS to a system with low contrast is very powerful for revealing structures in the intermediate length scale. The SR-SAXS measurements were performed by using the instrument installed on the beam line 10C of the Photon Factory, National Laboratory for High Energy Physics, Tsukuba, Ibaraki, Japan. The wavelength was 0.1488 nm. The range of h was 0.1–4 nm $^{-1}$. Exposure times of 200 s were used. The scattered X-ray signal was detected by using a one-dimensional position sensitive proportional counter. The scattering angle was calibrated by measuring the SAXS pattern of dried collagen as a standard. The details of the optics and instruments are given elsewhere.²⁰

The samples were contained in 20-mm-long pyrex tubes with internal and external diameters of 2.6 and 2.8 mm o.d. respectively. The concentrations of PBLG were 3.0 and 6.7 wt %. The temperature range was 10–41 $^{\circ}$ C for 3.0 wt % and 13–80 $^{\circ}$ C for 6.7 wt %, and each temperature indicated a constant temperature within 0.1 $^{\circ}$ C.

SR-SAXS Data Analysis. If aggregates of PBLG molecules in benzene behave as a long rod, the radius of gyration of the cross section, R_c , is then estimated from the scattered intensity of the cross section $\{hI(h)\}_c$ ²¹

$$\{hI(h)\}_c = I_c(0)\exp(-h^2 R_c^2/2), \quad hR_c < 1 \quad (1)$$

where $I_c(0)$ denotes the amount of scattering matter in the cross section on the absolute scale.

Results

Differential Scanning Calorimetry. The DSC traces on heating are shown in Figure 1. The DSC traces on heating exhibit two endotherms at about 25 $^{\circ}$ C and at about 30 $^{\circ}$ C,¹⁹ thereby indicating the melting of two types of aggregates. On the other hand, the DSC traces on cooling exhibit no exotherm in this concentration range even at 0 $^{\circ}$ C. This suggests that the PBLG solution is supercooled and it needs a time for the gelation. A hysteresis larger than approximately 25 $^{\circ}$ C was observed. Jackson and Shaw observed only a single DSC endotherm at about 27 $^{\circ}$ C for the gels formed by 1–10% PBLG in benzene,¹² although they observed the two-step decrease in rheological measurements for the solution of 1% PBLG in benzene. Our present result indicates that the sensitivity of their calorimeter was insufficient to detect two endotherms.

Figure 2 shows plots of the two peak positions (Figure 2a) and the two melting enthalpies (Figure 2b) as a function of PBLG concentration. As the concentration of PBLG increases, both melting temperatures slightly increase (Figure 2a), while the two melting enthalpies linearly increase with the concentration (Figure 2b). Since the number of aggregates indicating cross-linking points is proportional to the concentration, the bonding energy, proportional to the melting enthalpy divided by the concentration, is independent of the concentra-

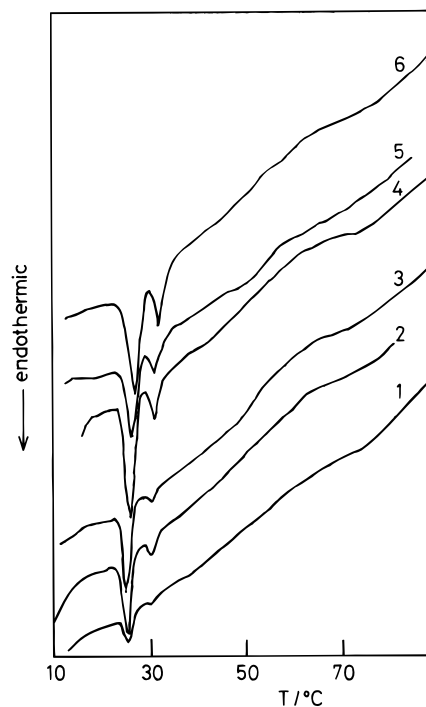


Figure 1. DSC traces for PBLG in benzene at a heating rate of 0.25 $^{\circ}$ C/min: 1 (1.0%), 2 (2.0%), 3 (3.0%), 4 (4.0%), 5 (5.0%), and 6 (7.7%). Solutions are cooled rapidly from 90 $^{\circ}$ C and annealed at 10 $^{\circ}$ C for 24 h.

tion.²² It is then noted that the slope of the melting enthalpy at about 25 $^{\circ}$ C is few times larger than that at about 30 $^{\circ}$ C, thereby suggesting that the bonding energy forming the aggregates at the lower transition is larger than that at the higher transition. However, the DSC result does not allow a distinction between solid crystalline or crystal-solvate phase.

Wide-Angle X-ray Diffraction. The WAXD profiles of a 20 wt % PBLG gel on heating as well as that of benzene at 23 $^{\circ}$ C are shown in Figure 3. These profiles yield little of interest other than diffuse halos from the solvent except SAXS in a range of h smaller than 4 nm $^{-1}$. The profile for liquid benzene shows three diffuse halos at spacings of 1.17 (a small peak), 0.597 (a large diffuse peak), and 0.39 nm (a shoulder), which are in a simple ratio of 1:1/2:1/3. The appearance of these spacings is considered to be an evidence that benzene molecules strongly interact with each other and behave as a cluster with an ordered structure observed in the solid benzene.²³ It is noted that a point of inflection at about 2.9 nm is observed in the profiles below 30 $^{\circ}$ C, and it disappears above 35 $^{\circ}$ C, indicating the disappearance of aggregates. Furthermore, a previous X-ray photograph of PBLG film cast from benzene showed a diffuse and weak diffraction ring, from which a degree of crystallinity of 8% was estimated.²⁴ Thus, WAXD results may be interpreted by the melting of the aggregates within a crystal-solvate phase. It is pointed out that a crystal-solvate phase is not necessarily poorly organized.²⁵

Small-Angle X-ray Scattering Using Synchrotron Radiation. The temperature variations of the Guinier plots of the cross section at two concentrations of 3.0 and 6.7 wt % are shown in Figures 4 and 5, respectively. Each Guinier plot shows a straight line at a limited range of h^2 , which was obtained with data points between the arrows in the figures by the least-squares method. On heating, both the initial slope and

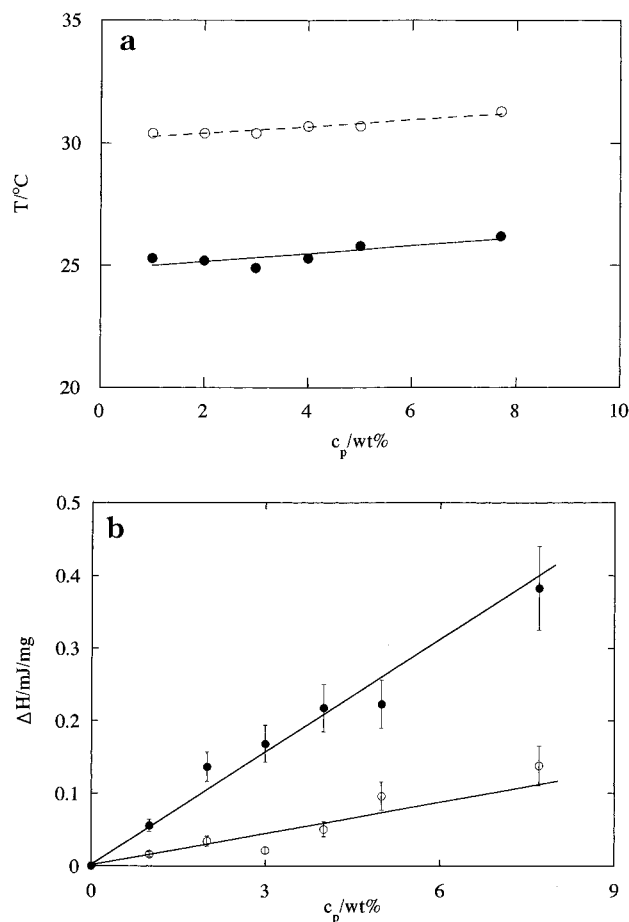


Figure 2. Plots of peak temperatures (a) and of melting enthalpies (b) of the transitions obtained on the heating of PBLG in benzene as a function of PBLG concentration.

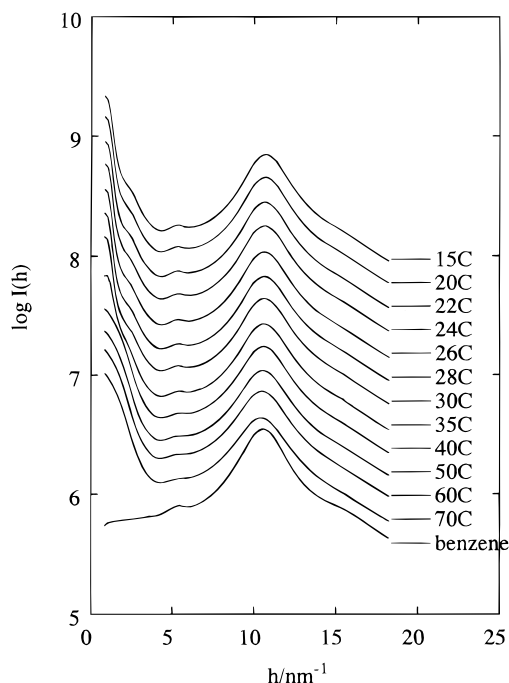


Figure 3. WAXD patterns for a 20 wt % PBLG in benzene.

the intercept at each concentration drastically decrease across the transition temperature at about 31 $^\circ\text{C}$. On the other hand, these values on cooling slightly decrease until 10 $^\circ\text{C}$ is reached, as shown in Figure 6.

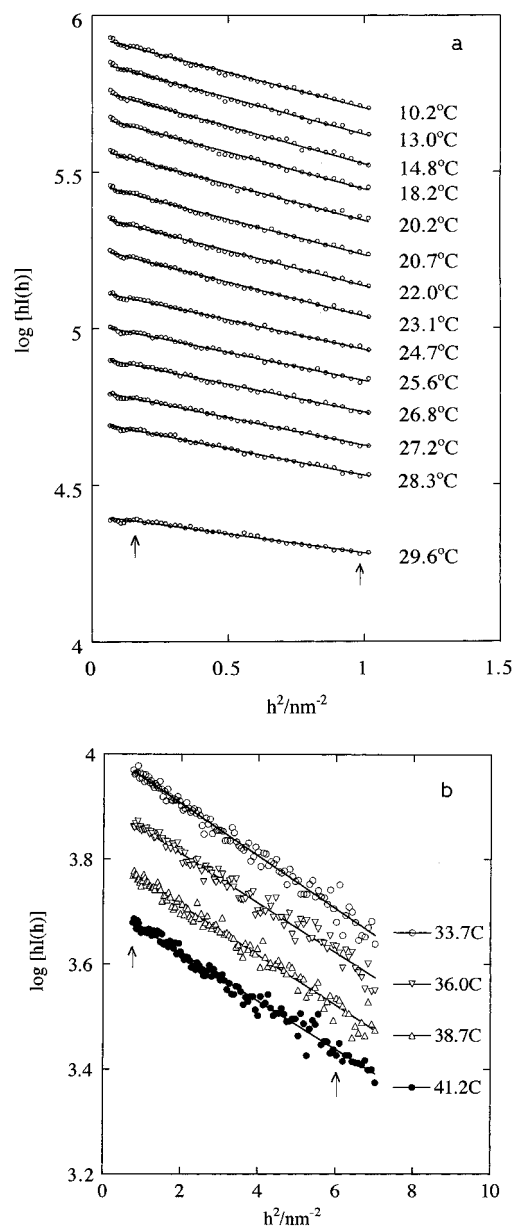


Figure 4. Temperature variations of the Guinier plots of the cross section for PBLG in benzene at a concentration of 3.0 wt %: (a) covering a range of temperature from 10.2 to 29.6 $^\circ\text{C}$; (b) covering a range of temperature from 33.7 to 41.2 $^\circ\text{C}$.

Parts a and b of Figure 6 show the temperature variations of the values of $I_c(0)$ and R_c estimated by applying eq 1 to each straight line indicated in Figures 4 and 5, respectively. It can be seen that the aggregates are almost formed by the side-by-side type, because the values of the cross sections of $I_c(0)$ and R_c at low temperature are clearly larger than those at high temperature. This result is in agreement with the previous result of electric birefringence.³⁻⁵ Both $I_c(0)$ and R_c decrease in two steps, indicating two-stage melting. The two-stage melting is observed at about 25 $^\circ\text{C}$ and at about 30 $^\circ\text{C}$ for both 3.0 and 6.7 wt % PBLG gels. It is noted that above the higher-temperature transition, the value of R_c does not depend on the concentration of PBLG and almost equals the radius of gyration of the cross section of a single α -helix of PBLG ($r_g = 0.48 \text{ nm}$).²⁶ A large hysteresis of approximately 22 $^\circ\text{C}$ was observed for the 6.7 wt % PBLG gel, in agreement with the result of large hysteresis observed in DSC measurements.

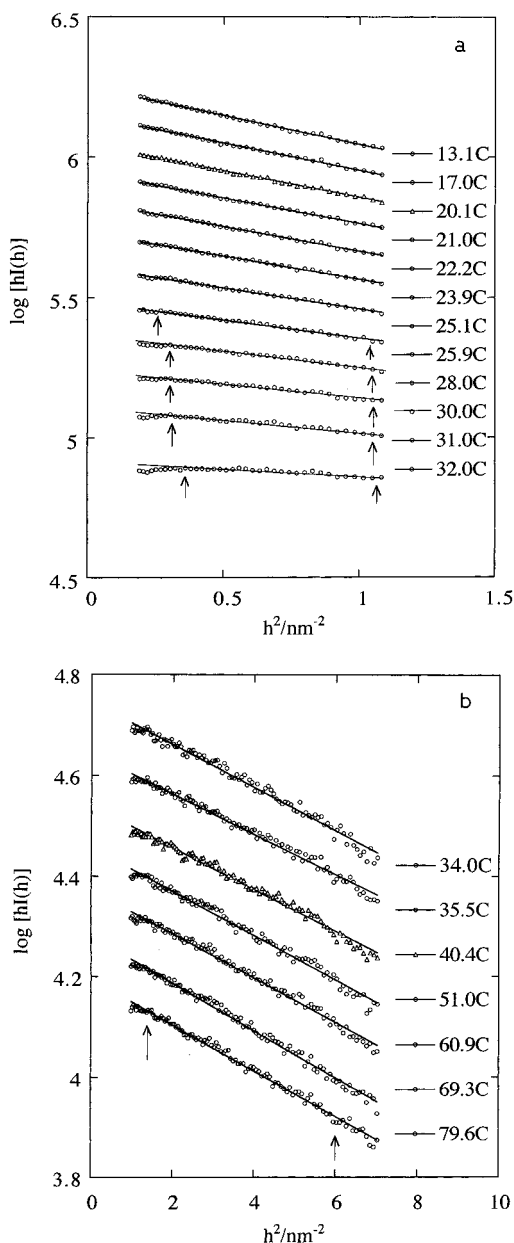


Figure 5. Temperature variations of the Guinier plots of the cross section for PBLG in benzene at a concentration of 6.7 wt %: (a) covering a range of temperature from 13.1 to 32.0 °C; (b) covering a range of temperature from 34.0 to 79.6 °C.

Discussion

We discuss the mechanism of the two-stage melting of the dilute gels based on the above results. DSC identified the melting of two aggregates. WAXD identified the microstructures of aggregates, in which they are composed of crystallike structure as in a co-crystal with solvent molecules. On the other hand, SAXS can characterize the structure in the intermediate length scales, between that of large-scale inhomogeneities and that of microstructures.

Mechanism of Two-Stage Melting Revealed by SR-SAXS. The present results of SR-SAXS support previous results that the PBLG in benzene aggregates side-by-side³⁻⁵ and indicate that the radius of gyration of the cross section of the aggregates in the dilute gel of 3 wt %, R_c , is about 1 nm below 25 °C, and as the temperature exceeds about 30 °C, it rapidly decreases from about 0.9 nm to about 0.48 nm. We assume that

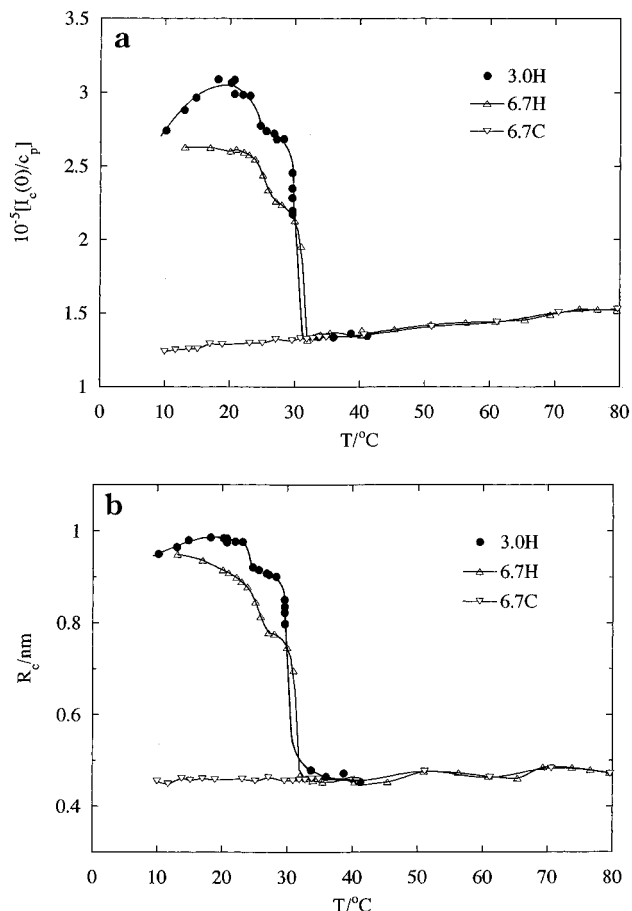


Figure 6. Temperature variations of the values of $I_c(0)/c_p$ (a) and R_c (b) for PBLG in benzene: 3.0H and 6.7H represent the samples of 3.0 and 6.7 wt % on heating, while 6.7C represents the sample of 6.7 wt % on cooling.

the aggregates can be approximated by an isolated assembly of parallel rods under the condition $R_c h < 1$. The expression for the intensity $I(h)$ is then given by introducing a swelling parameter γ defined by $d/(2(2^{1/2}) \cdot r_c)$,²⁷ in which d is the interrod spacing of PBLG and r_c is the radius of gyration of the cross section of single α -helix mentioned above

$$I(h) = (\pi \mu_L / h) [2J_1(\sqrt{2}hr_c) / \sqrt{2}hr_c]^2 T(2\sqrt{2}\gamma hr_c) \quad (2)$$

where μ_L is the mass per unit length of rod and $T(2(2^{1/2})\gamma hr_c)$, for the arrays of close-packed cylindrical rods having the number $N = 2 \sim 4$, is given by²⁸

$$T(x) = [2 + 2J_0(x)]/2^2 \quad \text{for } N = 2 \quad (3-1)$$

$$T(x) = [3 + 6J_0(x)]/3^2 \quad \text{for } N = 3 \quad (3-2)$$

$$T(x) = [4 + 10J_0(x) + 2J_0(x\sqrt{3})]/4^2 \quad \text{for } N = 4 \quad (3-3)$$

Here, J_0 and J_1 are the Bessel function of the first kind and, they are of zero and first order, respectively. By developing the Bessel functions in eqs 2 and 3 for $2^{1/2}hr_c < 1$ and $x < 1$, eq 2 reduces to

$$I(h) = (\pi \mu_L / h) \exp\{-h^2 r_c^2 [1 + 2\gamma^2/2]\} \quad \text{for } N = 2 \quad (4-1)$$

$$I(h) = (\pi\mu_L/h) \exp\{-h^2 r_c^2 [1 + 8\gamma^2/3]/2\} \quad \text{for } N=3 \quad (4-2)$$

$$I(h) = (\pi\mu_L/h) \exp\{-h^2 r_c^2 [1 + 4\gamma^2/2]\} \quad \text{for } N=4 \quad (4-3)$$

R_c in eq 1 is then given by

$$R_c^2 = r_c^2 [1 + 2\gamma^2] \quad \text{for } N=2 \quad (5-1)$$

$$R_c^2 = r_c^2 [1 + 8\gamma^2/3] \quad \text{for } N=3 \quad (5-2)$$

$$R_c^2 = r_c^2 [1 + 4\gamma^2] \quad \text{for } N=4 \quad (5-3)$$

Here, r_c can be evaluated from the radius of gyration of the cross section above the higher temperature transition, while R_c is evaluated from the value below the transition.

Table 1 compiles the calculated values of γ using eqs 5-1–5-3 for two values of R_c , 1.0 and 0.9 nm. Here, in evaluating γ , we used the data at 3.0 wt %, because the data at 6.7 wt % is largely influenced by the closer packing of the PBLG molecules. From the requirement of $\gamma > 1$, it is suggested that the maximum number of chains that participates in the formation of bundles is three. This result is not in agreement with the previous results,^{29–31} in which four chains participate in the formation of bundles but is in agreement with models in which three polymer chains passed through a unit cell. From Table 1, we select 1.12 as a critical value of γ for the determination of N , because the value of γ is always larger than 1, even if the value of 1.404 nm^{32,33} in the solid was used as the closest observed interrod distance. The aggregates characterized by $R_c = 1.0$ and 0.9 nm then correspond to bundles of three and two rods, respectively. Accordingly, one can attribute the present two-stage melting to a melting first of the bundles of three rods and then of the bundles of two rods. Instead of this, one may select a set of $\gamma = 1.29$ and 1.12, which means no change of N during the two-stage melting. Then, the two-stage melting may be explained by a partial melting of the cluster of benzene molecules. However, it seems to be difficult to adapt this idea for the explanation of the present results of DSC and WAXD.

The requirement of $\gamma > 1$ indicates that the benzene molecules are contained in the bundles of PBLG molecules. The aggregates of PBLG in benzene were previously characterized by side-by-side type with rods arranged in an antiparallel fashion.^{2–5} The aggregates of the side-by-side type may have some relation with the dielectric nature of solvent, considering the fact that the dielectric constants of the solvents having the aggregates of the side-by-side type are comparatively small.⁶ Therefore, it is suggested that an electrostatic interaction between the PBLG molecules via the benzene molecules may play an important role in this type of aggregation. Thus, the results of SAXS suggest that the cross-links can be formed by solvent induction. Furthermore, the solvent induction may explain the nature of the intermolecular interactions causing the bundles to aggregate.

Figure 7 shows a comparison between the experimental data at 20.7, 28.3, and 38.7 °C and the calculated curves for eq 4 with $R_c = 1.0, 0.9$, and 0.48 nm. The comparison is made by means of a Kratky plot, because, in this plot, the initial slope, the position of the

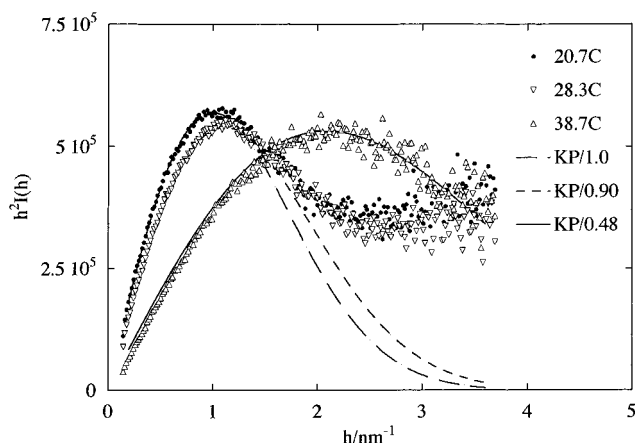


Figure 7. Kratky plots of $h^2 I(h)$ vs h for a 3.0 wt % PBLG in benzene at three different temperatures: 20.7, 28.3, and 38.7 °C. The broken, dashed, and solid lines stand for the calculation of eq 4 with $R_c = 1.0, 0.9$, and 0.48 nm, respectively.

Table 1. Values of the Swelling Parameter γ as a Function of the Number N of Rods

| N | γ | |
|-----|----------------|----------------|
| | $R_c = 1.0$ nm | $R_c = 0.9$ nm |
| 2 | 1.29 | 1.12 |
| 3 | 1.12 | 0.97 |
| 4 | 0.91 | 0.79 |

maximum of the intensity, and the width of this maximum impose very severe checks on the present analysis. As can be seen, the experimental data can be satisfactorily explained by the application of eq 4. The result suggests that there is only one radius in the present gels. A deviation from eq 4 observed for the data at 20.7 and 28.3 °C in a range of h larger than 1.5 nm⁻¹ will be explained in the following section. On the other hand, Guenet et al. observed in poly(methyl methacrylate) gels that the radius found in the Guinier range was in fact the superposition of two different radii arising from two structures.^{34,35} It is suggested that the structures of the present gels may be different from theirs.

In the presence of the correlation between different bundles, eq 2 is generalized by introducing a radial distribution function $g(r)$ ²⁷

$$I(h) = (\pi\mu_L/h) [2J_1(\sqrt{2}hr)/\sqrt{2}hr_c]^2 T(2\sqrt{2}\gamma hr_c) \{1 - 2\pi n \int r [1 - g(r)] J_0(hr) dr\} \quad (6)$$

in which n is the number of bundles per unit area.

If the bundles are separated by a distance $d_{bb} > R_c$, then there is a domain ($d_{bb}^{-1} < h < R_c^{-1}$) where, by considering $g(r) = 0$ and developing the Bessel function for $hr > 1$, eq 6 reduces to^{36,37}

$$I(h) = (\pi\mu_L/h) \exp(-h^2 R_c^2/2) [1 - 2\pi n h^{-0.5} f(hd_{bb})] \quad (7)$$

in which $f(hd_{bb})$ is an oscillating function. For $hd_{bb} \gg 1$, eq 7 plotted by means of a Kratky representation tends to^{36,37}

$$h^2 I(h) = Ah + B \quad (8)$$

in which A and B are constants depending on $f(hd_{bb})$. It is also noted that a maximum occurs in the Kratky plot of eq 7 for $hd_{bb} < 1$, though the location obviously

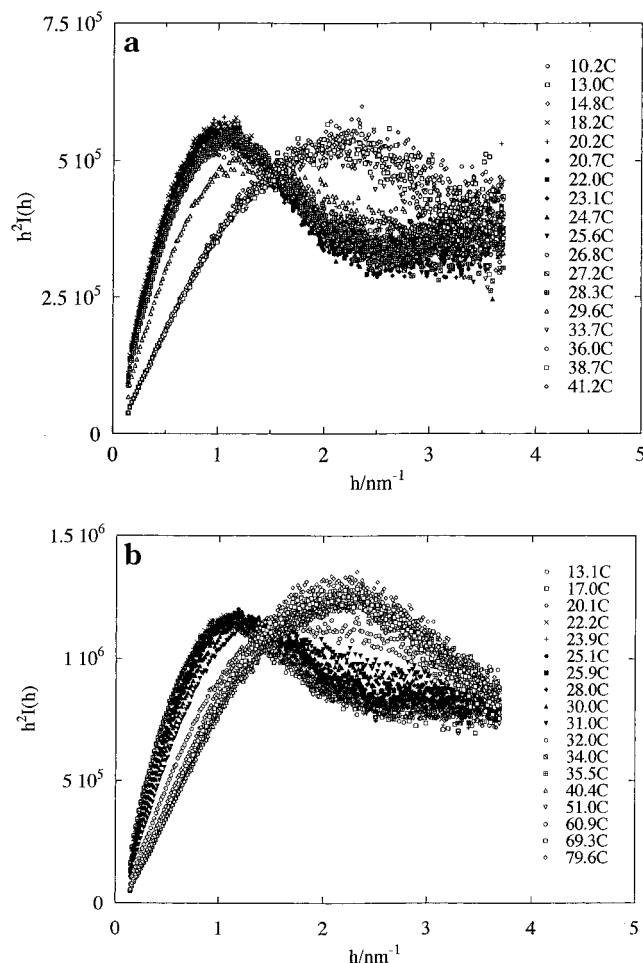


Figure 8. Kratky plots of $h^2 I(h)$ vs h for PBLG in benzene at two concentrations of 3.0 (a) and 6.7 wt % (b).

depends on $f(hd_{bb})$. These predictions agree well with what is found experimentally below the transition at higher-temperature as shown in parts a and b of Figure 8.

Conclusions

The two-stage melting of the dilute gels of poly(γ -benzyl L-glutamate) in benzene is not puzzling. That is, DSC measurements show that the traces on heating exhibit two distinct endothermic peaks at about 25 °C and at about 31 °C, thereby indicating the melting of two types of aggregates, while those on cooling exhibit no exotherm even at 0 °C, thereby indicating a large thermal hysteresis. WAXD measurements show that the profiles yields little of interest other than diffuse halos from the solvent except a shoulder at spacing of about 2.4 nm, thereby indicating the melting of the aggregates with a crystal-solvate phase. SR-SAXS measurements show that the two-stage melting of the aggregates can be attributed to a melting first of the bundles of three rods and then of the bundles of two rods and that, above the two-stage melting temperature, the gels transform into the dilute and isotropic solutions, in which the PBLG stiff chains are randomly dispersed and do not interact with each other. As a result, the

intermolecular interactions causing the bundles to aggregate are induced by the solvent.

Acknowledgment. We thank Prof. K. Kobayashi of Photon Factory for his help in the measurements of SAXS. This work has been performed with the approval of the Photon Factory Advisory Committee (Proposal No. 93G244). This work was partly supported by a Grant-in-Aid (Proposal No. 09875239) from the Ministry of Education, Science, and Culture, Japan.

References and Notes

- (1) Doty, P.; Bradbury, J. H.; Holtzer, A. M. *J. Am. Chem. Soc.* **1956**, *78*, 947.
- (2) Wada, A. *J. Polym. Sci.* **1960**, *45*, 145.
- (3) Watanabe, H. *J. Chem. Soc. Jpn.* **1965**, *86*, 179.
- (4) Powers, J. C., Jr.; Peticolas, W. L. *Biopolymers* **1970**, *9*, 195.
- (5) Kihara, H. *Polym. J.* **1977**, *9*, 443.
- (6) Sakamoto, R. *Rep. Prog. Polym. Phys. Jpn.* **1980**, *22*, 699.
- (7) Ushiki, H.; Mita, I.; *Polym. J.* **1984**, *16*, 751; **1985**, *17*, 1297.
- (8) Tohyama, K.; Miller, W. G. *Nature* **1981**, *289*, 813.
- (9) Sasaki, S.; Tokuma, K.; Uematsu, I. *Polym. Bull.* **1983**, *10*, 539.
- (10) Uematsu, I.; Uematsu, Y. *Adv. Polym. Sci.* **1984**, *59*, 37.
- (11) Hill, A.; Donald, A. M. *Polymer* **1988**, *29*, 1426.
- (12) Jackson, C. L.; Shaw, M. T. *Polymer* **1990**, *31*, 1070.
- (13) Horton, J. C.; Donald, A. M. *Polymer* **1991**, *32*, 2418.
- (14) Shukla, P. *Polymer* **1992**, *33*, 365.
- (15) Prystupa, D. A.; Donald, A. M. *Macromolecules* **1993**, *26*, 1947.
- (16) Cohen, Y.; Dagan, A. *Macromolecules* **1995**, *28*, 7638.
- (17) Tipton, D. L.; Russo, P. S. *Macromolecules* **1996**, *29*, 7402.
- (18) Tsutsumi, A.; Hikichi, K.; Takahashi, T.; Yamashita, Y.; Matsushima, N.; Kanke, M.; Kaneko, M. *J. Macromol. Sci.* **1973**, *B8*, 413.
- (19) Izumi, Y.; Kikuta, N.; Tsutsumi, A. *Rep. Prog. Polym. Phys. Jpn.* **1993**, *36*, 515.
- (20) Ueki, T.; Hiragi, Y.; Izumi, Y.; Tagawa, H.; Kataoka, M.; Muroga, Y.; Matsushita, T.; Amemiya, Y. *KEK Progress Report 83-1, Photon Factory Activity Report; 1982/1983*, pp VI-70. Tsukuba; Ueki, T.; Hiragi, Y.; Kataoka, M.; Inoko, Y.; Amemiya, Y.; Izumi, Y.; Tagawa, H.; Muroga, Y. *Biophys. Chem.* **1985**, *23*, 115.
- (21) Glatter, O. In *Small Angle X-ray Scattering*; Glatter, O., Kratky, O., Eds.; Academic Press: New York, 1982; Chapter 4.
- (22) Watase, M.; Nishinari, K.; Clark, A. H.; Ross-Murphy S. B. *Macromolecules* **1989**, *22*, 1196.
- (23) Narten, A. H. *J. Chem. Phys.* **1968**, *48*, 1630.
- (24) Fukuzawa, T.; Uematsu, I. *Polym. J.* **1974**, *6*, 431.
- (25) Daniel, C.; De Luca, M. D.; Brulet, A.; Menelle, A.; Guenet, J.-M. *Polymer* **1996**, *37*, 1273.
- (26) Saludjian, P.; Luzzati, V. *J. Mol. Biol.* **1966**, *15*, 681.
- (27) Oster, G.; Riley, D. P. *Acta Crystallogr.* **1952**, *5*, 272.
- (28) Vainshtein, B. K. *Diffraction of X-rays by Chain Molecules*; Elsevier Pub.: Amsterdam, 1966; Chapter 6.
- (29) Fukuzawa, T.; Uematsu, I.; Uematsu, Y. *Polym. J.* **1974**, *6*, 431.
- (30) Watanabe, J.; Kishida, H.; Uematsu, I. *Polym. Prepr. Jpn.* **1981**, *30*, 279.
- (31) Sasaki, S.; Hikata, M.; Shiraki, C.; Uematsu, I. *Polym. J.* **1982**, *14*, 205.
- (32) Bamford, C. H.; Elliott, A.; Hanby, W. E. *Synthetic Polypeptides*; Academic Press: New York, 1956; p 263.
- (33) Parry, D. A. D.; Elliott, A. *J. Mol. Biol.* **1967**, *25*, 1.
- (34) Fazel, N.; Brulet, A.; Guenet, J.-M. *Macromolecules*, **1994**, *27*, 3836.
- (35) Saiani, A. Guenet, J.-M. *Macromolecules* **1997**, *30*, 966.
- (36) Guenet, J.-M. *Thermoreversible gelation of polymers and biopolymers*; Academic Press: New York, 1992; Chapter 2.
- (37) Klein, M.; Brulet, A.; Guenet, J.-M. *Macromolecules* **1990**, *23*, 540.

MA9708609